SUPPORTING INFORMATION

Small-molecule procaspase-3 activation sensitizes cancer to treatment with diverse chemotherapeutics

Rachel C. Botham, Howard S. Roth, Alison P. Book, Patrick J. Roady, Timothy M. Fan and Paul J. Hergenrother*

TABLE OF CONTENTS

Supporting Figure 1

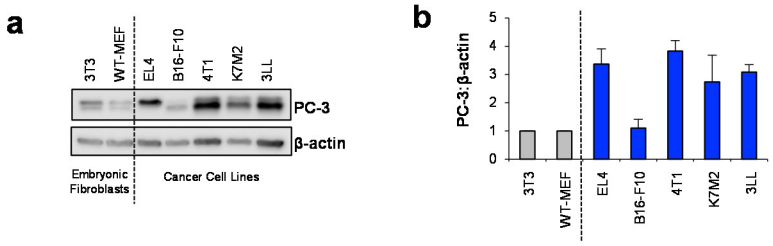

Supporting Figure 1. Procaspase-3 is overexpressed in cancerous murine cell lines. **(a)** The expression of procaspase-3 in murine embryonic fibroblasts and cancerous cell lines was determined by immunoblotting. **(b)** Quantification of relative procaspase-3 expression compared to β-actin for murine embryonic fibroblasts and cancerous cell lines (n = 3 biologic replicates, error bars show SEM).

Supporting Figure 2

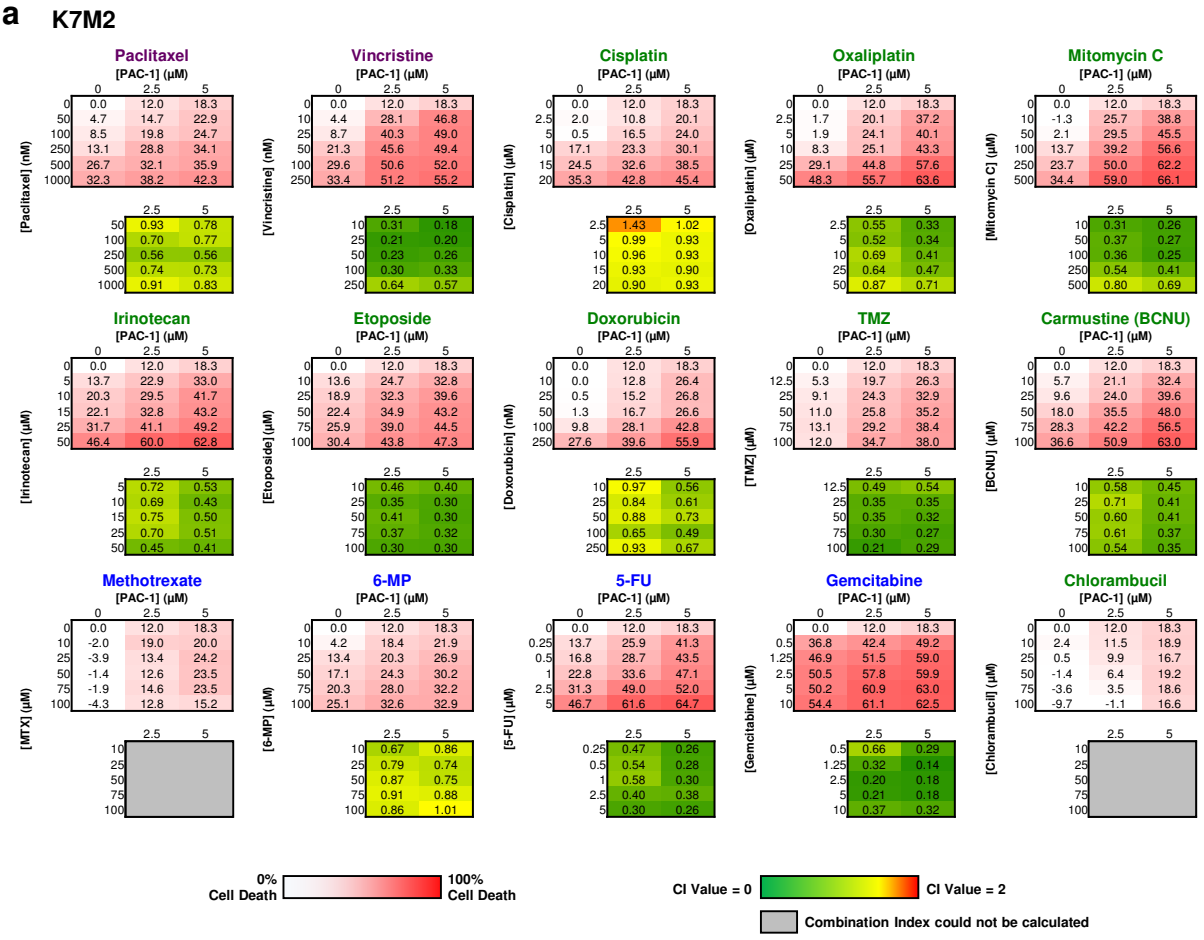

Supporting Figure 2. The combination of PAC-1 and conventional chemotherapeutics was evaluated for the ability to synergistically induce death in a panel of murine cancer cell lines. In the survey, combinations were evaluated in 3x6 concentration matrices, and each was quantified for synergy using the Chou-Talalay combination index method (CI values). Murine cancer cell lines K7M2 **(a),** EL4 **(b),** B16-F10 **(c),** 4T1 **(d),** and 3LL **(e)** were evaluated. Three independent biologic replicates were performed, the average of those is shown. Calculation of CI values is only possible when agents induce positive and increasing levels of cell death across a range of increasing concentrations.

Supporting Figure 2 (continued)

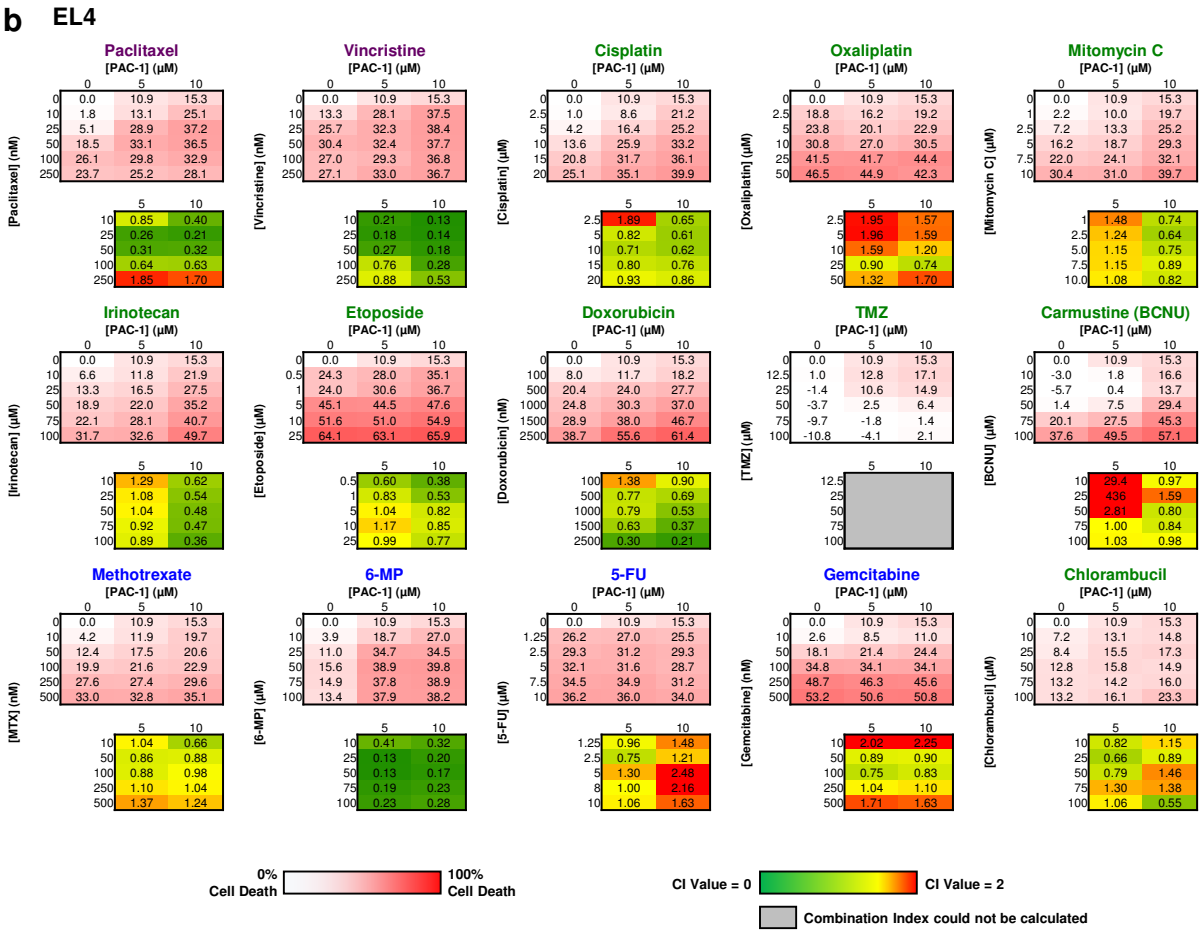

Supporting Figure 2 (continued)

C **B16-F10**

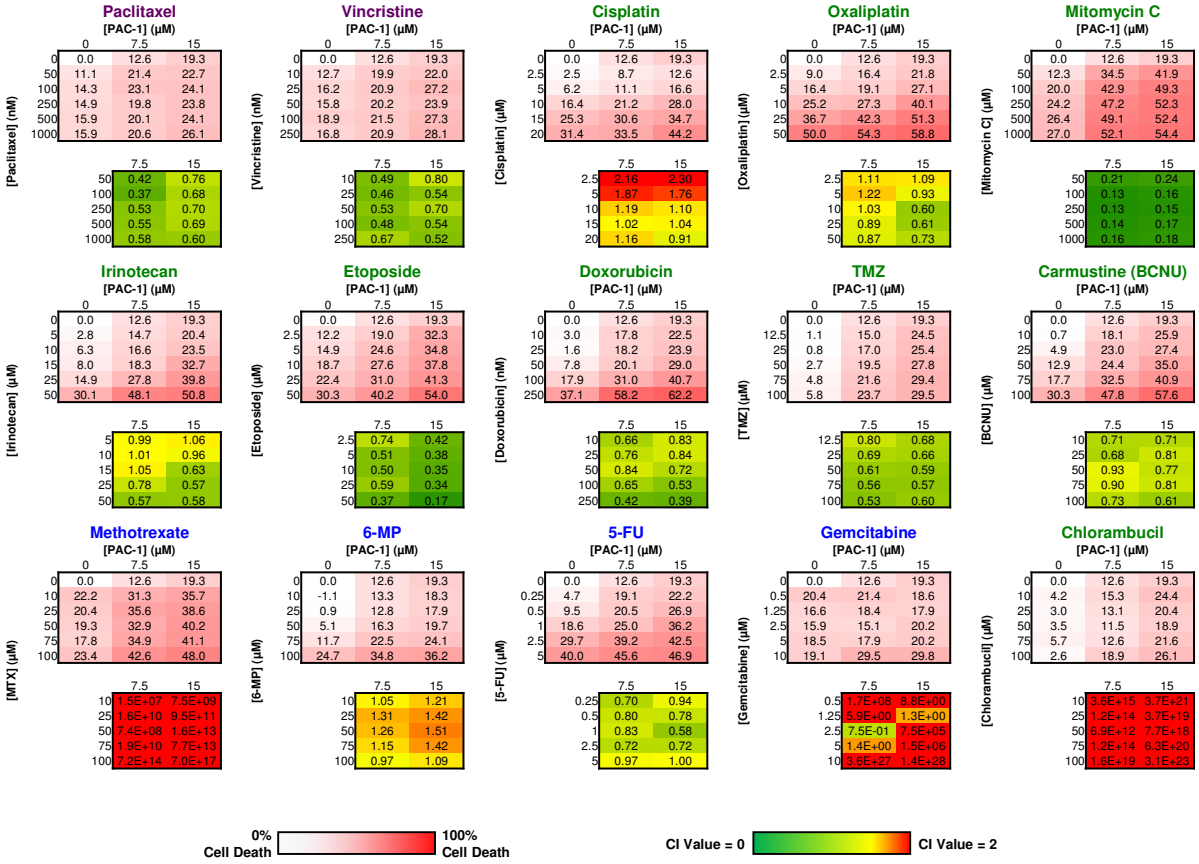

Supporting Figure 2 (continued)

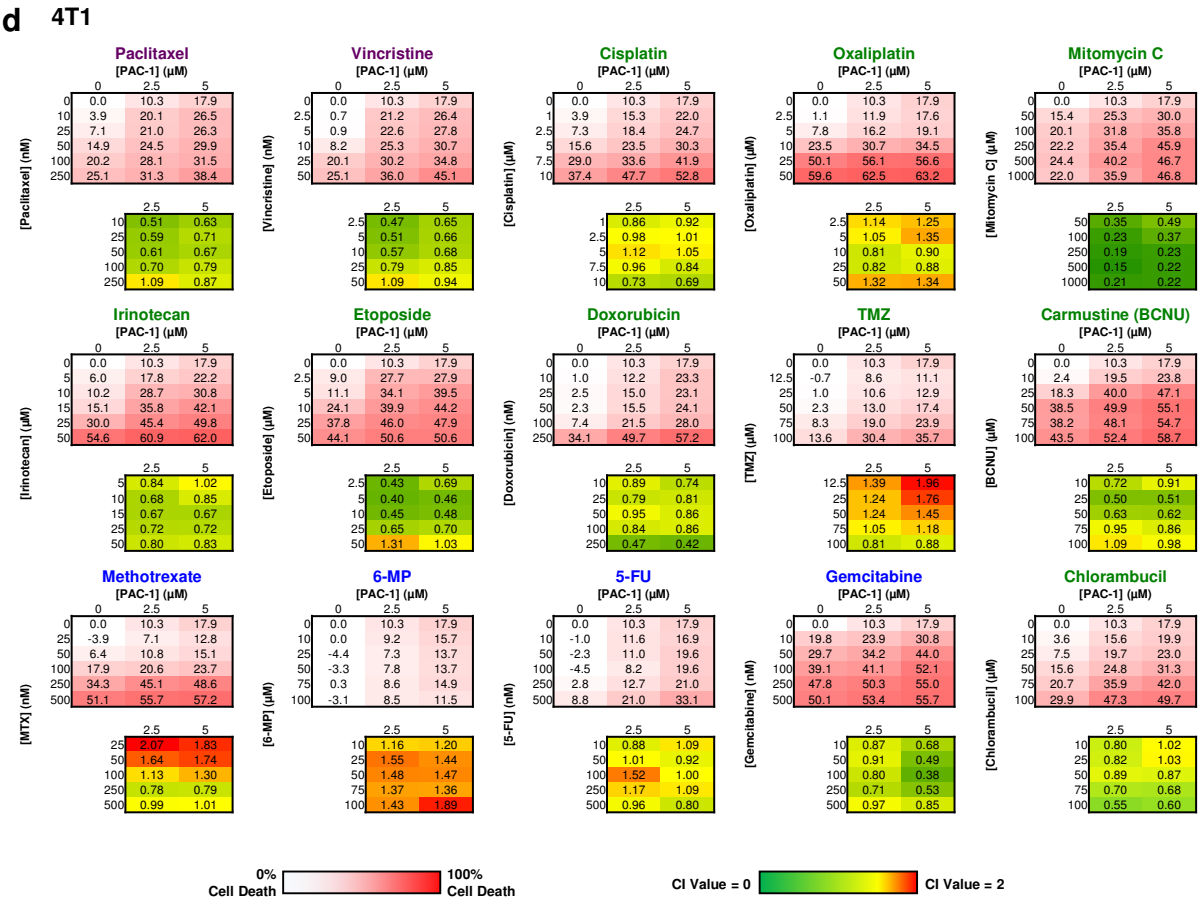

Supporting Figure 2 (continued)

e **3LL**

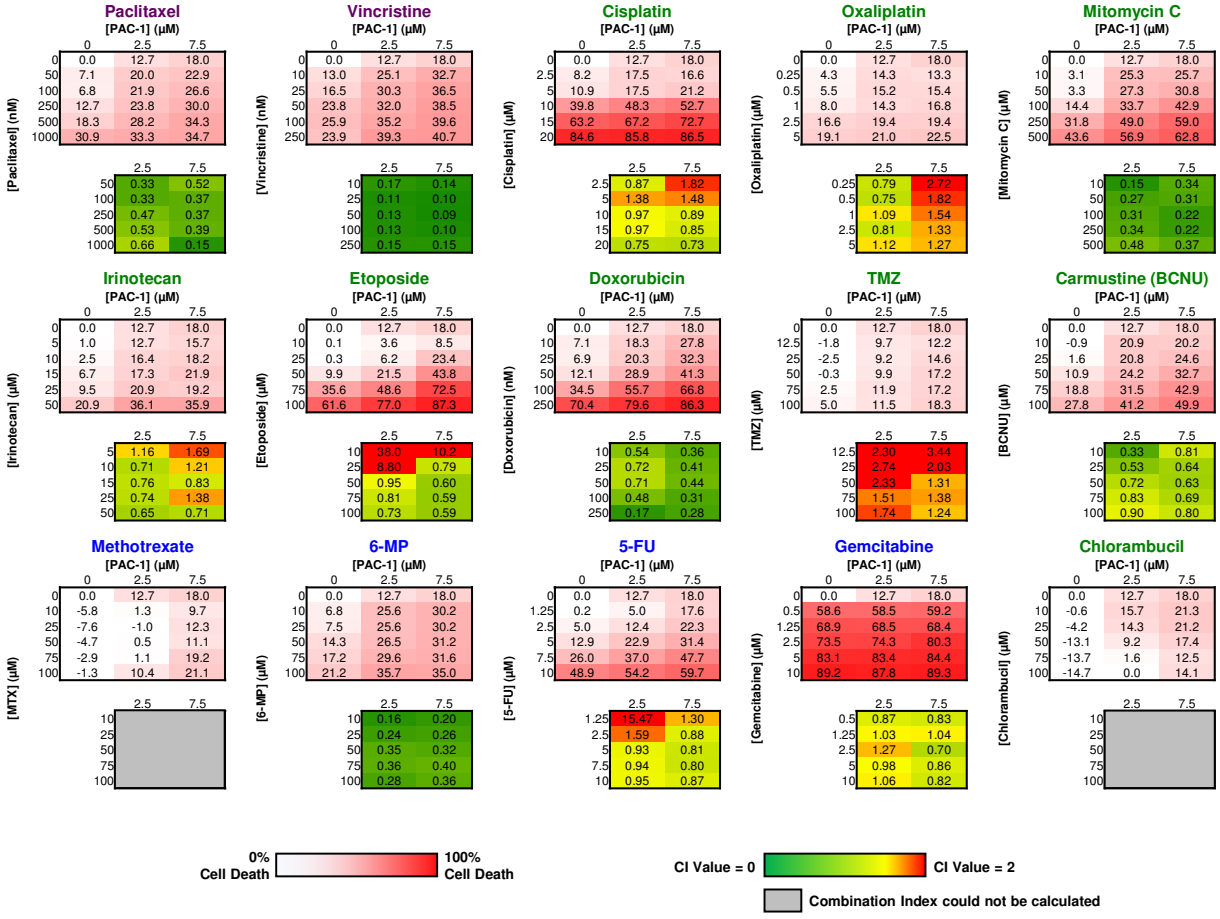

Supporting Figure 3

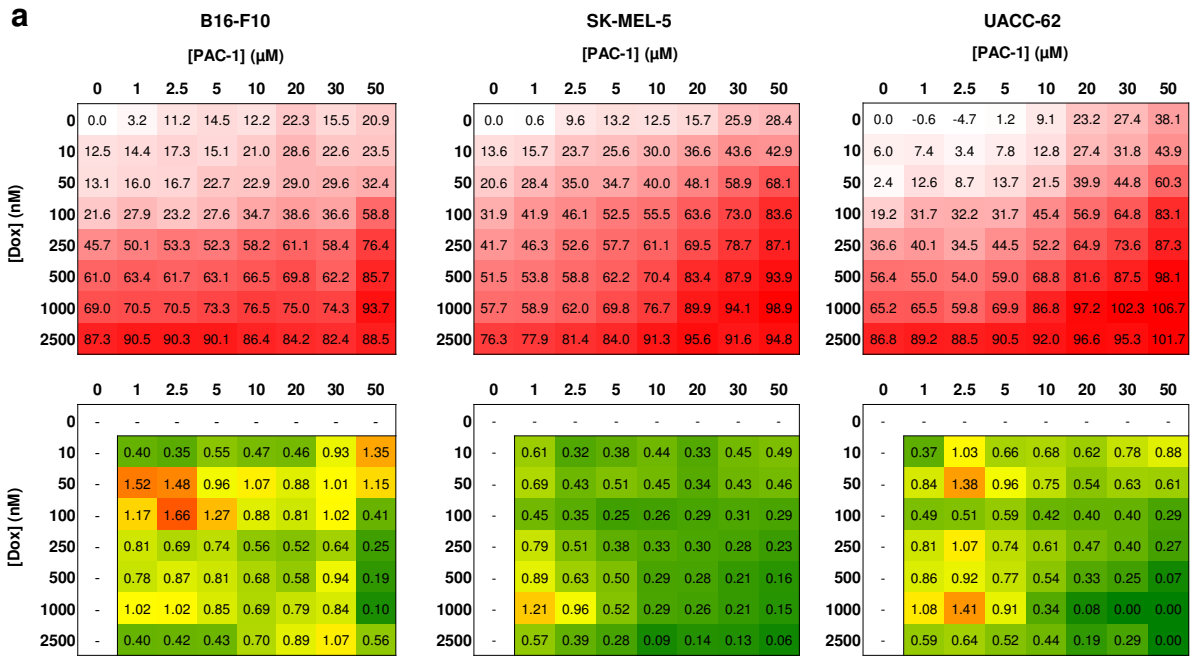

Supporting Figure 3. The combination of PAC-1 and doxorubicin is strongly synergistic in murine and human cancers. Cell death and CI value quantification for 8x8 matrices of PAC-1 and doxorubicin in murine and human melanoma **(a)**, breast cancer **(b)**, and lung cancer **(c),** (n ≥3 biologic replicates).

Supporting Figure 3 (continued)

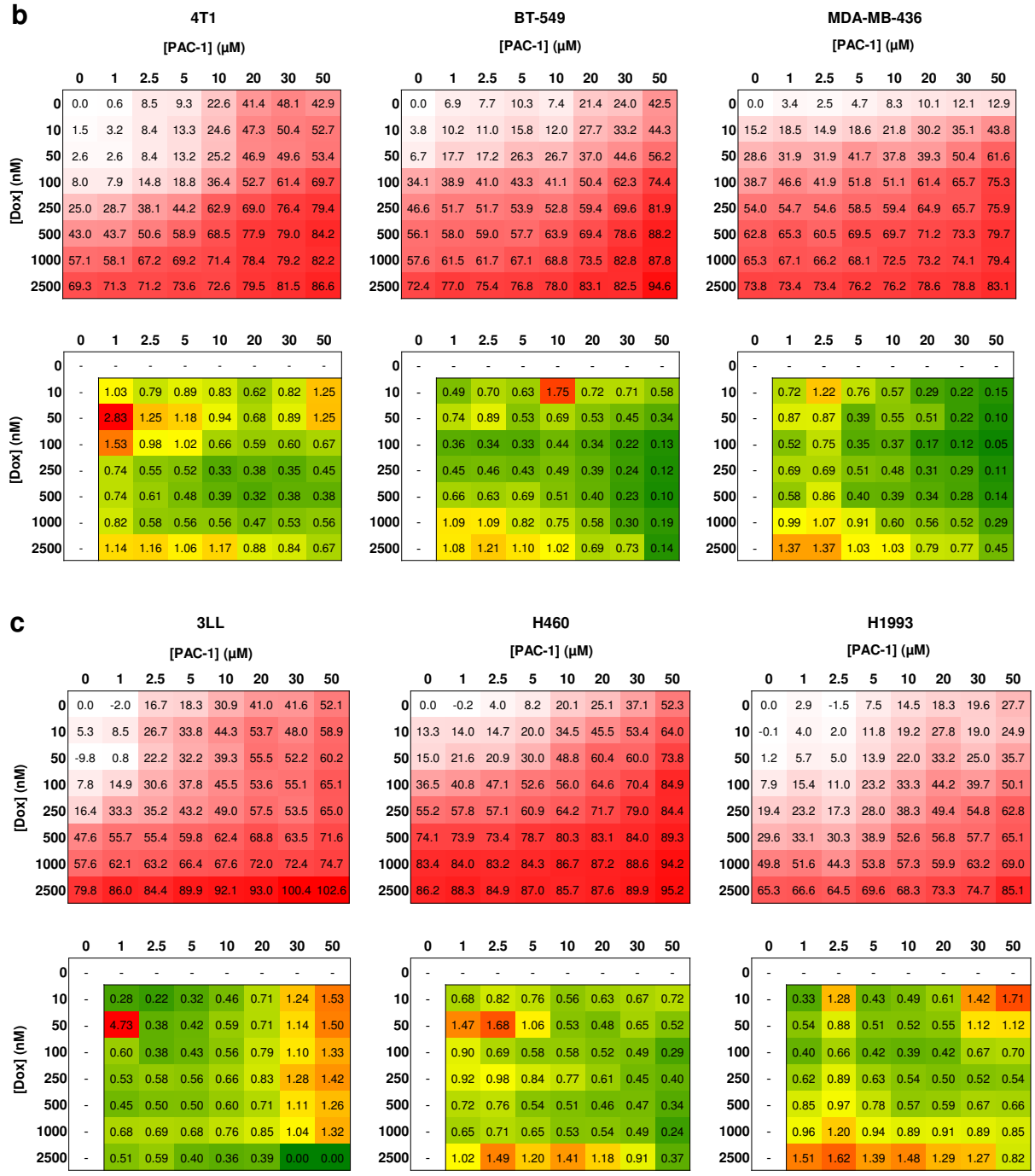

Supporting Figure 4

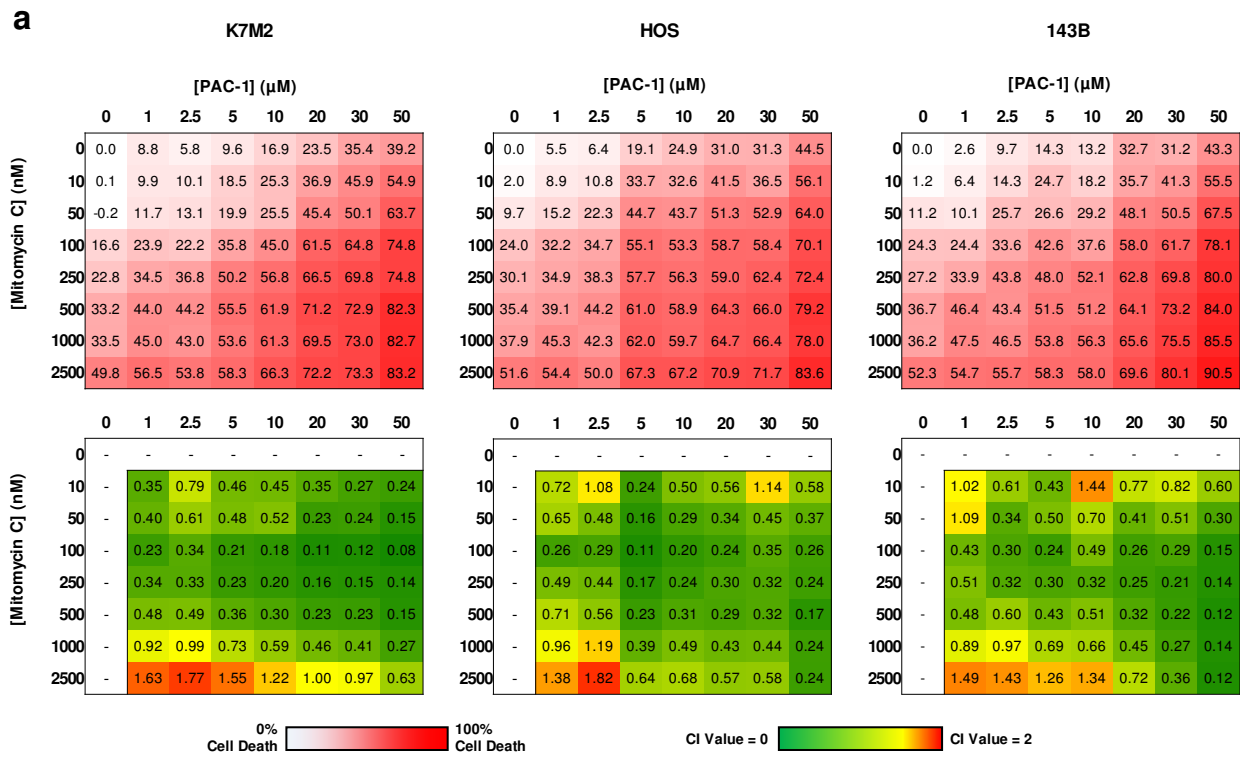

Supporting Figure 4. The combination of PAC-1 and mitomycin C is strongly synergistic in murine and human cancers. Cell death and CI value quantification for 8x8 matrices of PAC-1 and doxorubicin in murine and human osteosarcoma **(a)**, melanoma **(b),** breast cancer **(c)**, and lung cancer **(d),** (n ≥3 biologic replicates).

Supporting Figure 4 (continued)

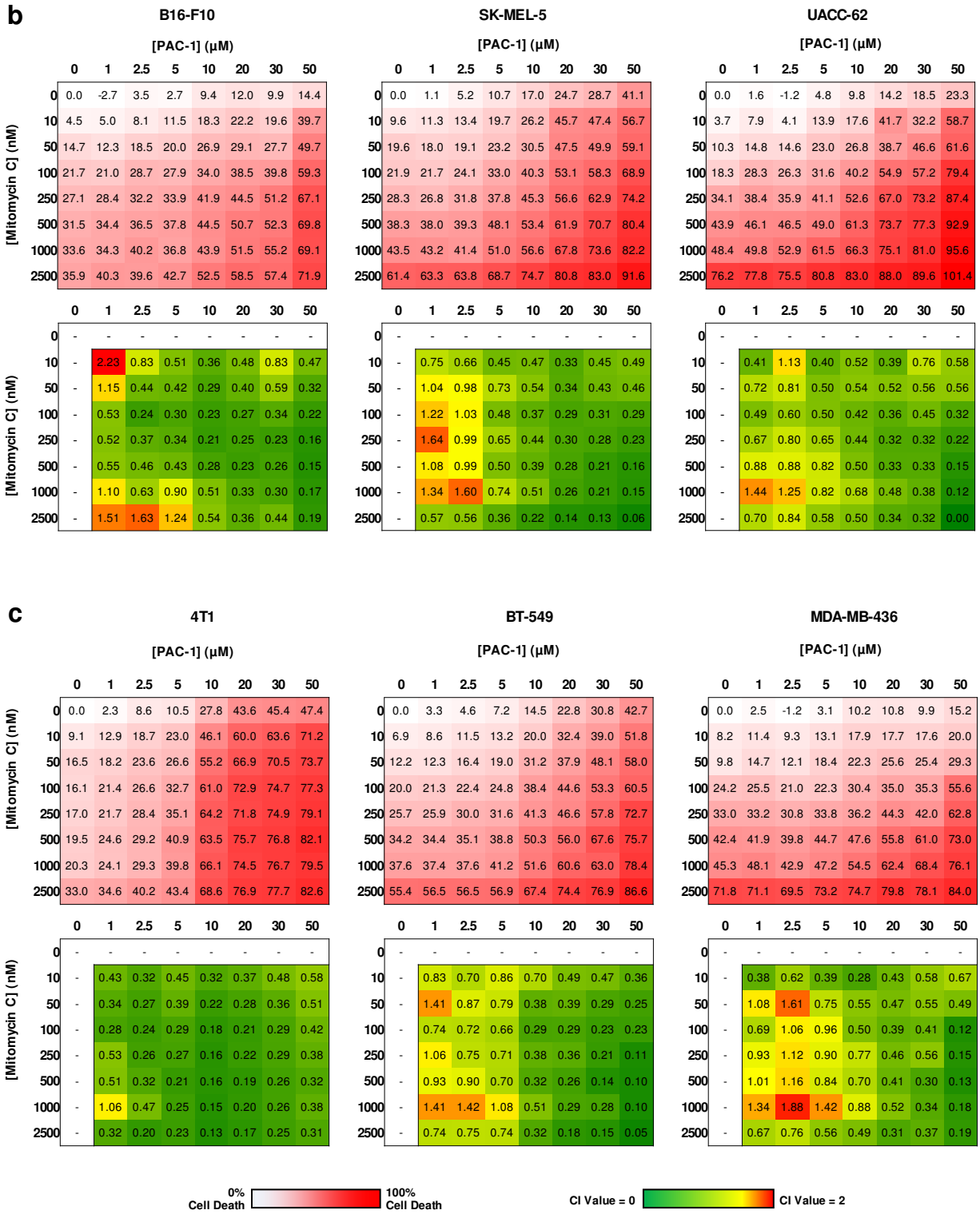

Supporting Figure 4 (continued)

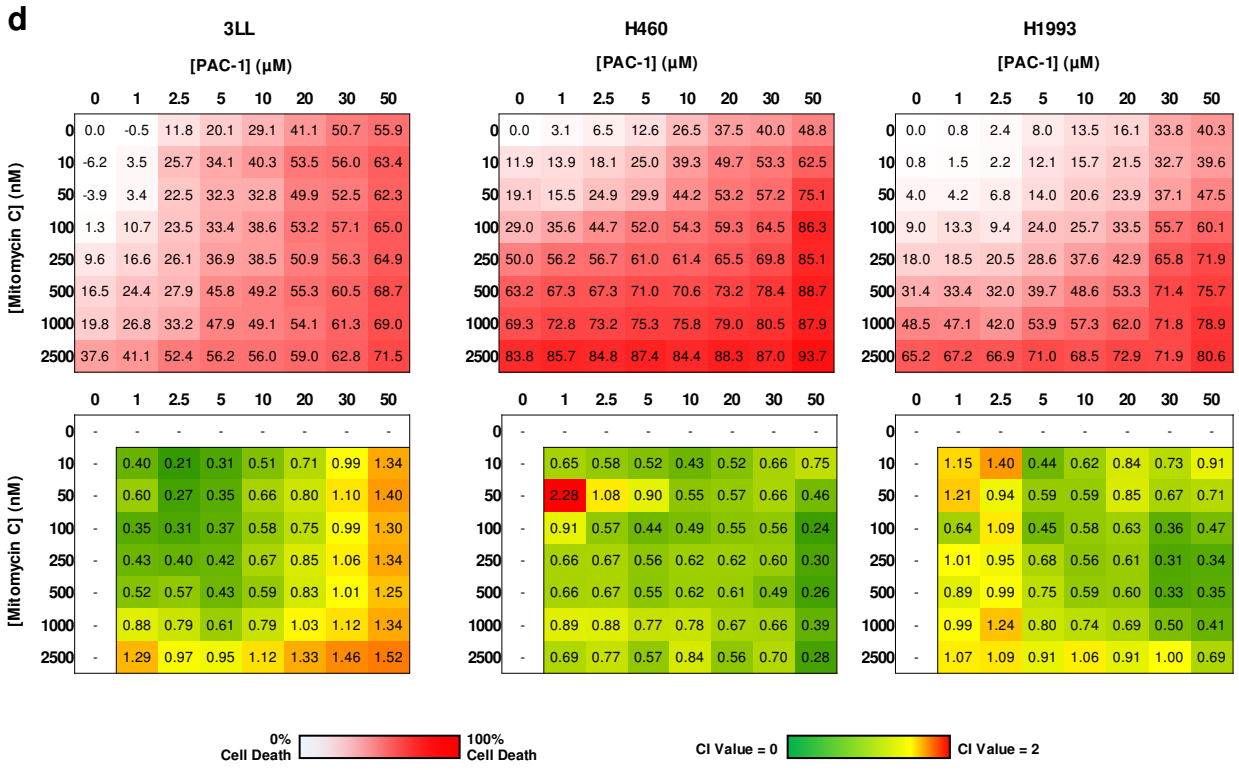

Supporting Figure 5

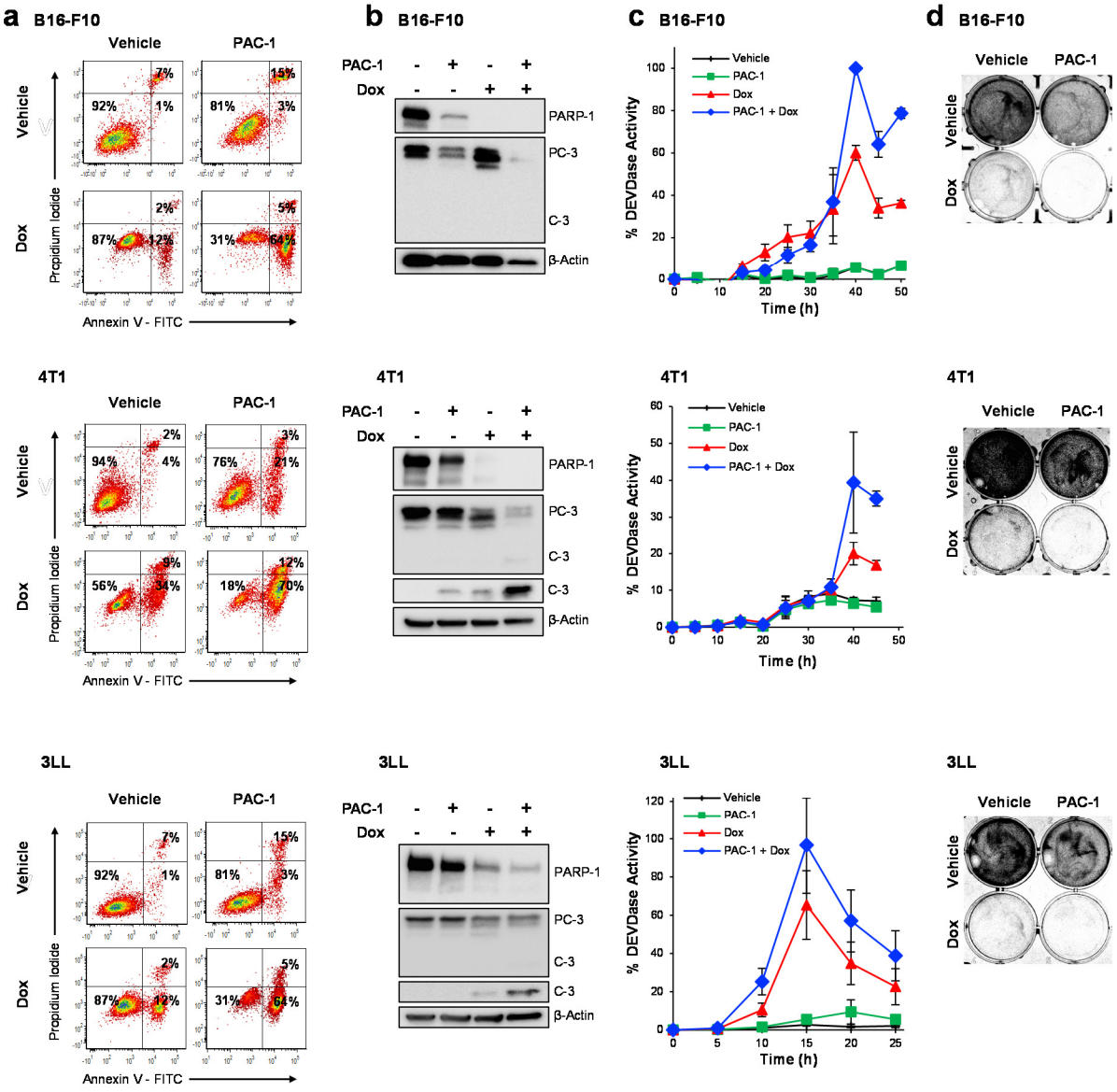

Supporting Figure 5. The combination of PAC-1 and doxorubicin induces apoptosis in murine cancer cell lines. Cancer cell lines B16-F10 (top panels), 4T1 (middle panels), and 3LL (bottom panels) were treated with vehicle, PAC-1 (B16-F10: 10 µM, 4T1: 7.5 µM, 3LL: 10 µM), doxorubicin (B16-F10: 0.75 µM, 4T1: 1 µM, 3LL: 1 µM), or the combination of PAC-1 + doxorubicin, and evaluated for **(a)** induction of apoptosis by Annexin V-FITC and propidium iodide staining (B16-F10, 4T1: 48 h treatment, 3LL: 24 h treatment), **(b)** by Western blot analysis for cleavage of markers of apoptosis procaspase-3 and PARP-1 (B16-F10, 4T1: 48 h treatment, 3LL: 24 h treatment), and **(c)** for executioner caspase activity over time (n ≥3 biologic replicates, error bars show SEM) **(d)** Adherent B16-F10, 4T1 and 3LL cells were stained for qualitative comparison of biomass following treatment (B16-F10, 4T1: 48 h treatment, 3LL: 24 h treatment). Annexin V-FITC/propidium iodide plots, Western blots, and caspase activity time course evaluations are representative of at least three independent biologic experiments. *See Figure 3 for analogous evaluations of PAC-1 and doxorubicin in osteosarcoma and lymphoma.*

Supporting Figure 6

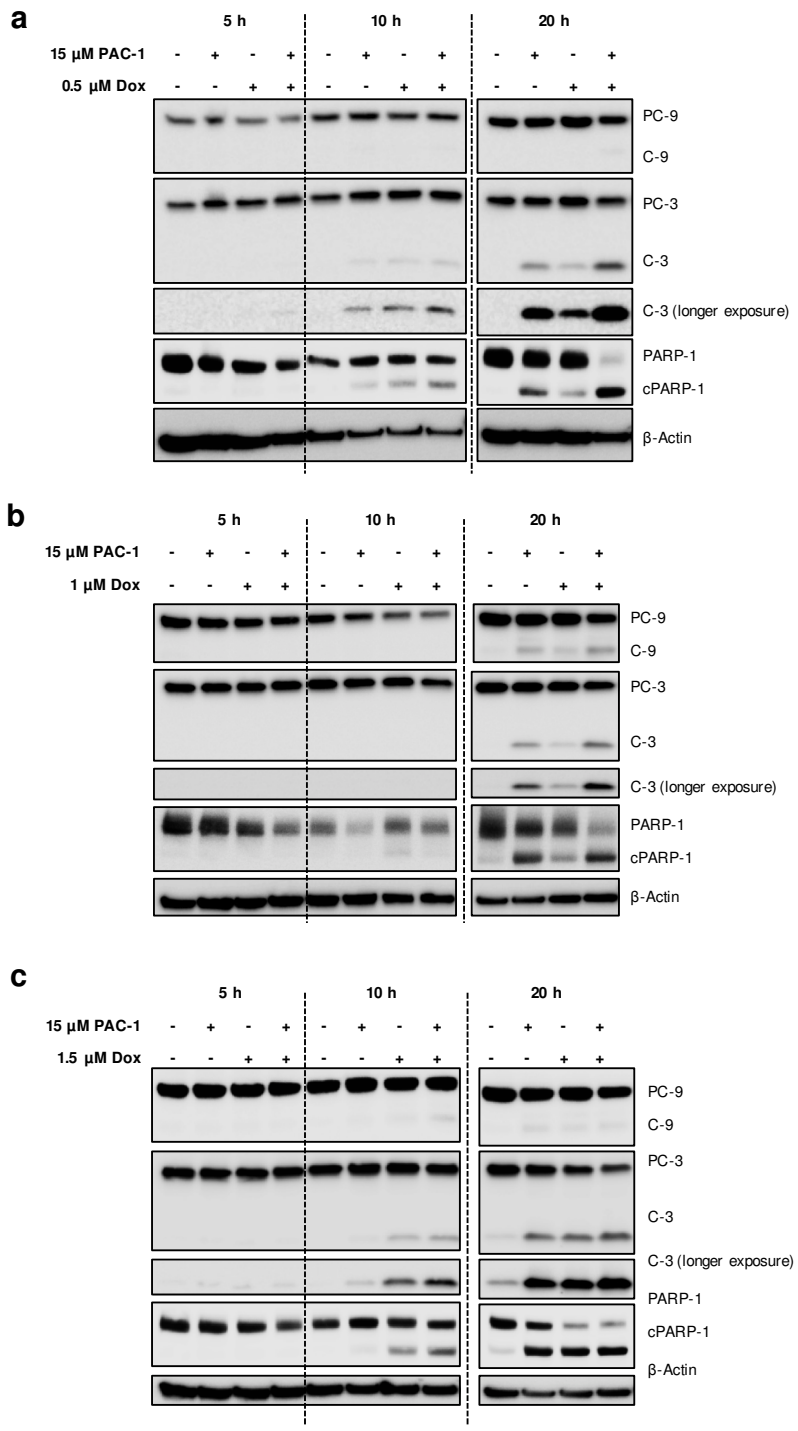

Supporting Figure 6. PAC-1 synergistically enhances doxorubicin-induced apoptosis in EL4 murine lymphoma cells. Executioner caspase activity was monitored by examining cleavage of PARP-1. Cells were treated with PAC-1 (15 µM) in combination with three concentrations of doxorubicin: (**a**) 0.5 µM, (**b**) 1 µM, and (**c**) 1.5 µM, thereby varying the strength of doxorubicin-induced pro-apoptotic assault.

Supporting Figure 7

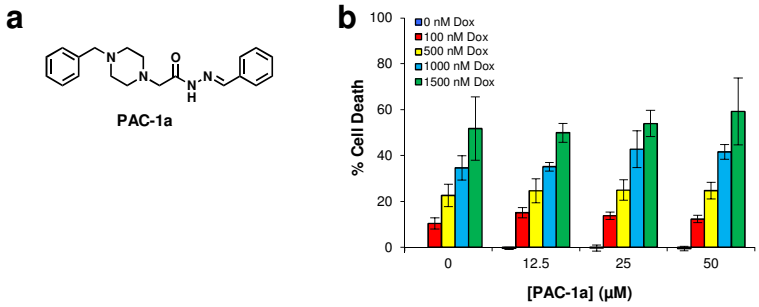

Supporting Figure 7. Inactive derivative PAC-1a does not synergize with doxorubicin in EL4 murine lymphoma cells **(a)** Structure of PAC-1a. **(b)** Cells were treated with the indicated concentrations of PAC-1a and doxorubicin for 24 h and apoptotic cell death was assessed by flow cytometry with Annexin V-FITC and propidium iodide staining. Three independent biologic replicates were performed, error bars show SD.

Supporting Figure 8

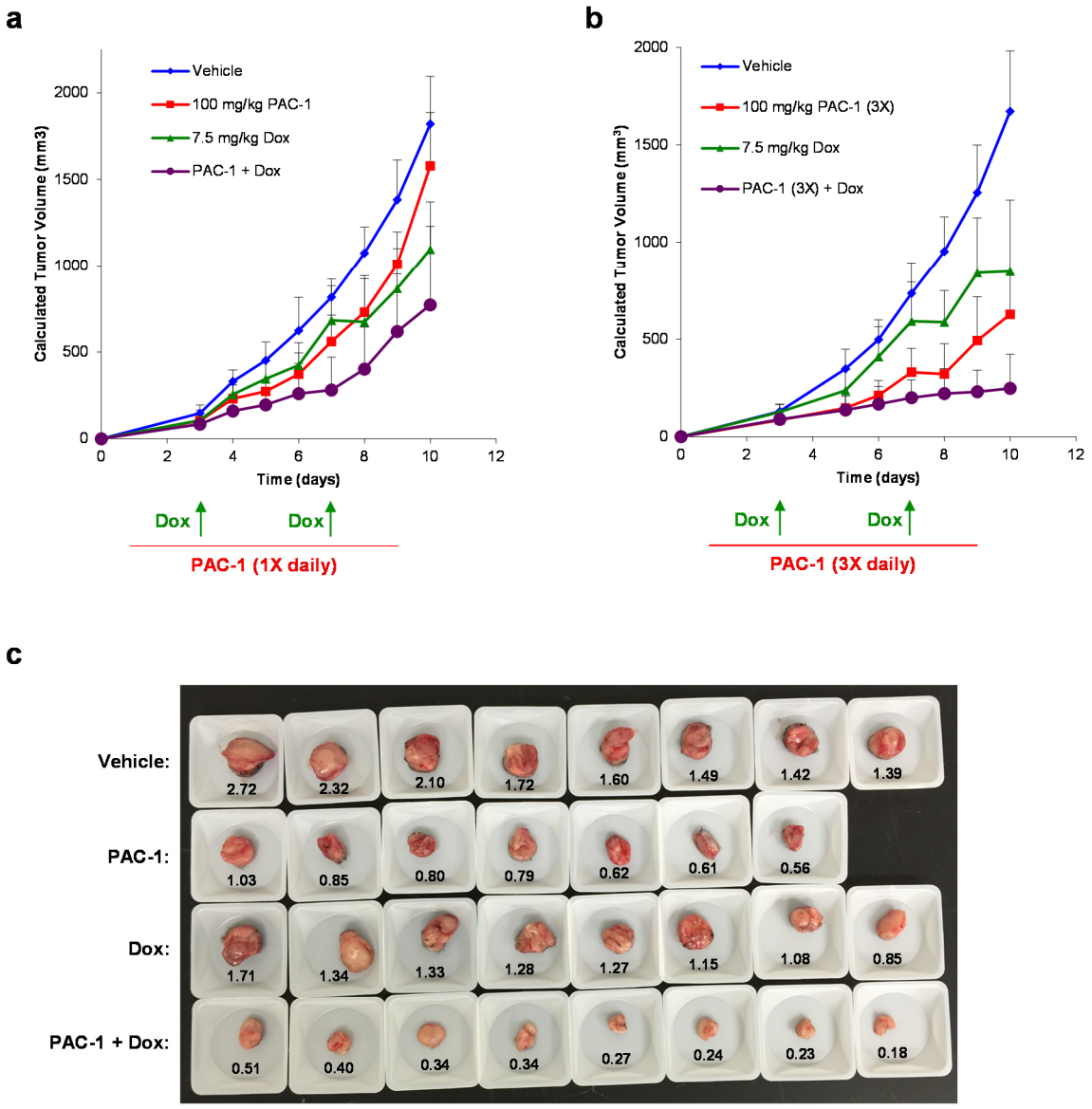

Supporting Figure 8. The combination of PAC-1 and doxorubicin has an antitumor effect in murine models of lymphoma. PAC-1, doxorubicin and PAC-1 + doxorubicin were evaluated in two syngeneic subcutaneous EL4 murine lymphoma models. **(a)** EL4 inoculated mice were treated with PAC-1 once-daily (Days 1-9, 100 mg/kg, IP, in HPβCD), with doxorubicin (Days 3 and 7, 7.5 mg/kg, IP, in 0.9% saline) or with vehicles. Tumors were measured with calipers beginning on day 3 and total tumor volume was calculated as $(l \times w^2)/2$. Tumor volume over time is shown, error bars show SD. **(b, c)** EL4 inoculated mice were treated with PAC-1 thrice-daily (Days 1-9, 100 mg/kg, IP, in HPβCD), with doxorubicin (Days 3 and 7, 7.5 mg/kg, IP, in 0.9% saline) or with vehicles. Tumors were measured with calipers beginning on day 3 and total tumor volume was calculated as $(l \times w^2)/2$. Tumor volume over time is shown, error bars show SD. After ten days the mice were sacrificed and the tumors excised and weighed. Numbers shown below each tumor indicate the weight in grams. *Tumor images associated with Figure 4d and Supporting Figure 8b.*

Supporting Figure 9

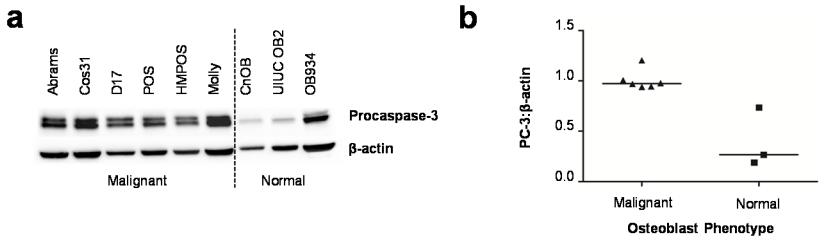

Supporting Figure 9. Procaspase-3 is overexpressed in canine osteosarcoma. **(a)** The expression of procaspase-3 in canine osteoblasts and cancerous cell lines was determined by immunoblotting. **(b)** Quantification of relative procaspase-3 expression compared to β-actin for canine osteoblasts and cancerous cell lines.

Supporting Figure 10

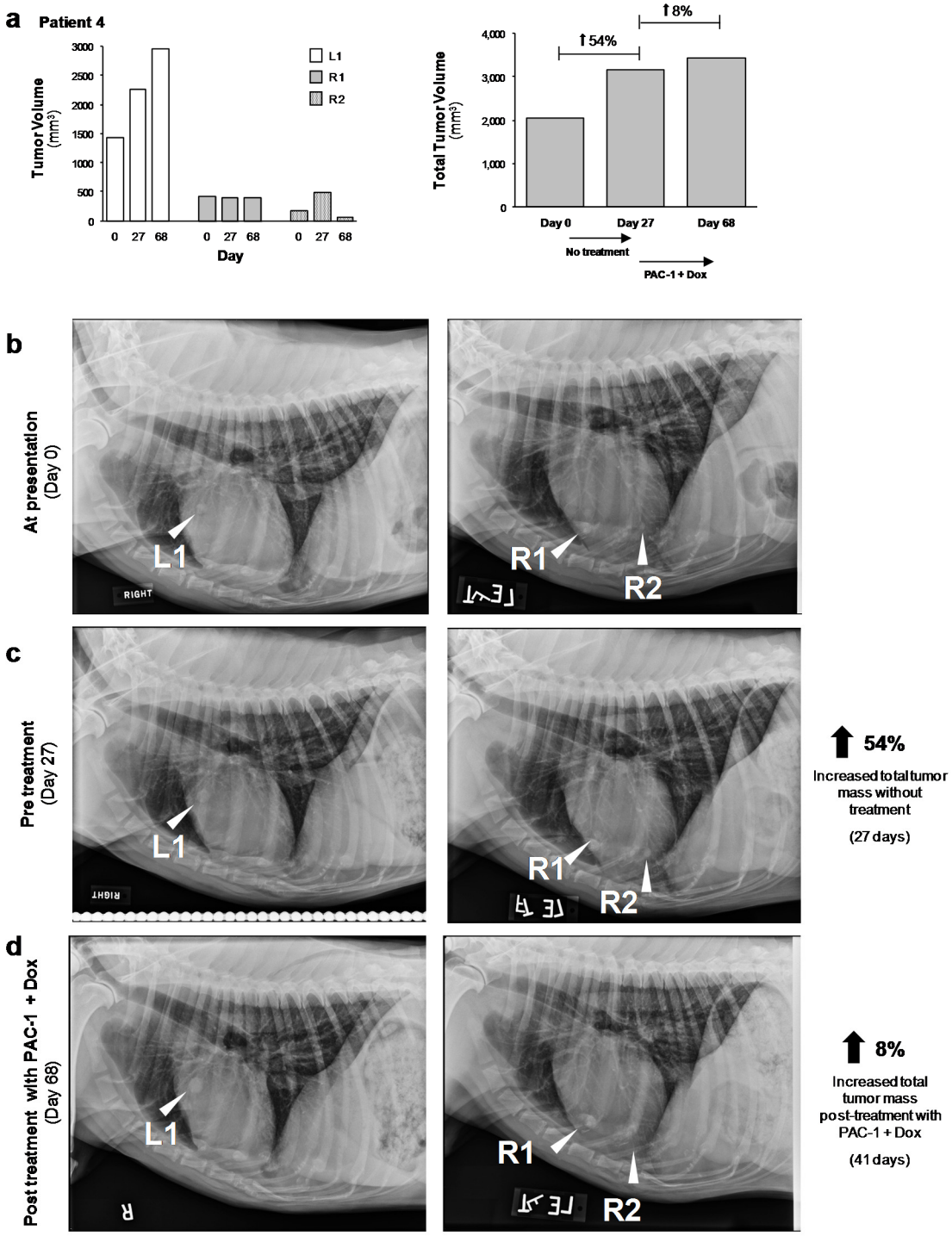

Supporting Figure 10. Activity of PAC-1 + doxorubicin in osteosarcoma Patient 4. **(a)** A pet dog (Patient 4) presented with rapidly growing, drug-naïve osteosarcoma, with three measurable masses. Patient 4 was treated daily with 11.5 mg/kg PAC-1 (PO), and 25 mg/m^2 doxorubicin on days 27, 41 and 55. Chest films of masses L1, R1 and R2 at presentation **(b),** after 27 days without treatment **(c)**, and after treatment with PAC-1 and doxorubicin (Day 68) **(d).**

Supporting Figure 11

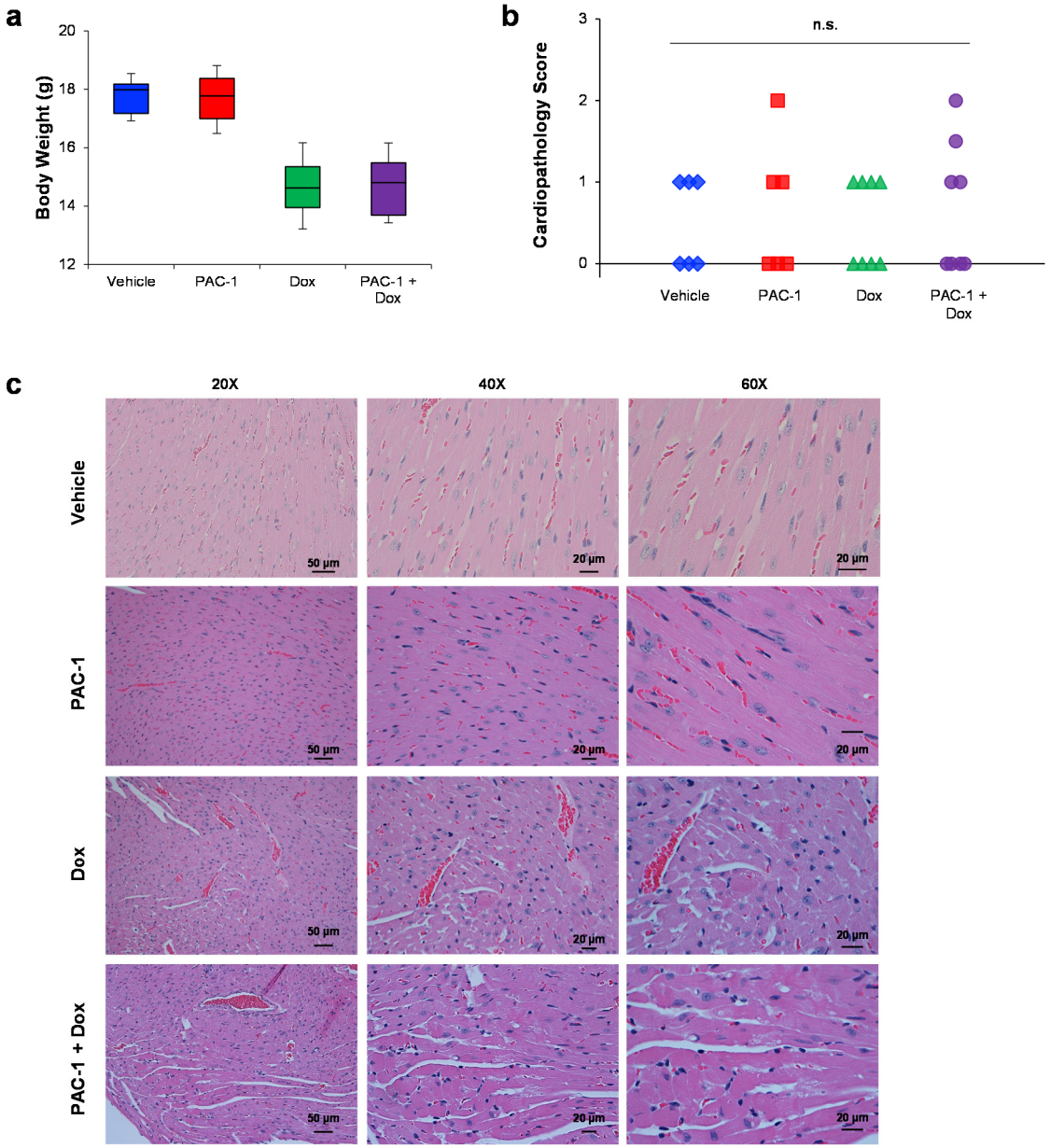

Supporting Figure 11. PAC-1 does not enhance doxorubicin-mediated toxicity *in vivo*. BALB/C mice were treated with PAC-1 (daily from days 1 and 15, 125 mg/kg, oral, in HPβCD), with doxorubicin (days 5 and 10, 7.5 mg/kg, IV, in 0.9% saline) or with vehicles. n = 6-8 mice per group. Mice were sacrificed on Day 16 and **(a)** body mass was determined. **(b)** Hearts were excised and stained with hematoxylin-eosin. Alterations were evaluated semi-quantitatively by light microscopy analysis of sections and scored from 0 to 3, based on the percentage of myocytes displaying myofibrillar loss and cytoplasmic vacuolization: 0, no alteration; 1, <5%; 1.5, 5%-15%; 2.0, 16%-25%; 2,5, 26%-35%; and 3, >35% of the myocardial cells showing damage. **(c)** Representative images of hematoxylin-eosin stained hearts from each treatment group are shown at 20X, 40X and 60X magnification. Scale bars are shown in each image.

Supporting Table 1. Hematologic tolerability of canine cancer patients treated with PAC-1 + doxorubicin

Patient	Cancer Type	White Blood Cells ($x10^3$ cells/μL)	Neutrophils ($x10^3$ cells/μL)	Platelets ($x10^3$ cells/μL)	Hematocrit (%)
	Reference range:	6-17.0 x 10^3	3-11.5 x 10^3	200-900 x 10^3	35-52%
1	Osteosarcoma	9.7 ± 1.4	6.6	395.3 ± 91.2	38.6 ± 0.5
2	Osteosarcoma	10.5 ± 0.4	8.7 ± 0.4	311.7 ±136.0	45.0 ± 1.5
3	Osteosarcoma	11.3 ± 1.9	7.6 ± 0.1	467.3 ± 69.0	47.5 ± 2.3
4	Osteosarcoma	10.6 ± 1.0	ND	299.0 ± 32.5	45.2 ± 0.7
5	Osteosarcoma	10.8 ± 0.2	ND	557.7 ± 59.4	39.5 ± 0.8
6	Osteosarcoma	9.8 ± 1.5	ND	314.0 ± 60.6	47.7 ± 1.7
7	Lymphoma	5.9 ± 0.9	4.1 ± 0.9	232.7 ± 119.5	49.0 ± 4.6
8	Lymphoma	11.1 ± 0.6	ND	395.0 ± 103.1	45.9 ± 2.7
9	Lymphoma	7.4 ± 2.2	ND	475.7 ± 86.8	38.9 ± 1.3
10	Lymphoma	11.4 ± 3.3	ND	248.3 ± 95.3	33.0 ± 6.7

Abbreviation: ND, not determined